Hydrogeol J (2015) 23:1745–1759
DOI 10.1007/s10040-015-1311-9

REPORT

Groundwater evolution and recharge determination of the Quaternary aquifer in the Shule River basin, Northwest China

Jianhua He[1] · **Jinzhu Ma**[1] · **Wei Zhao**[1] · **Shuang Sun**[1]

Received: 11 February 2015 / Accepted: 24 August 2015 / Published online: 11 September 2015

Abstract Groundwater recharge and evolution in the Shule River basin, Northwest China, was investigated by a combination of hydrogeochemical tracers, stable isotopes, and radiocarbon methods. Results showed the general chemistry of the groundwater is of SO_4^{2-} type. Water–rock reactions of halite, Glauber's salt, gypsum and celestite, and reverse ionic exchange dictated the groundwater chemistry evolution, increasing concentrations of Cl^-, Na^+, SO_4^{2-}, Ca^{2+}, Mg^{2+} and Sr^{2+} in the groundwater. The $\delta^{18}O$ and δ^2H values of groundwater ranged from −10.8 to −7.7 and −74.4 to −53.1 ‰, respectively. Modern groundwater was identified in the proluvial fan and the shallow aquifer of the fine soil plain, likely as a result of direct infiltration of rivers and irrigation returns. Deep groundwater was depleted in heavy isotopes with ^{14}C ages ranging from 3,000 to 26,000 years, suggesting palaeowater that was recharged during the late Pleistocene and middle Holocene epochs under a cold climate. These results have important implications for groundwater management in the Shule River basin, since large amounts of groundwater are effectively being mined and a water-use strategy is urgently needed.

Keywords Stable isotopes · Radiocarbon · Groundwater evolution · Recharge · China

Electronic supplementary material The online version of this article (doi:10.1007/s10040-015-1311-9) contains supplementary material, which is available to authorized users.

✉ Jianhua He
hjh_hi@126.com

[1] Key Laboratory of Western China's Environmental System (Ministry of Education), College of Earth and Environmental Sciences, Lanzhou University, 222 South Tianshui Road, Lanzhou 730000, China

Introduction

Groundwater is an important component of global freshwater resources. More than 1.5 billion people worldwide rely on groundwater as their primary source of drinking water (Clarke et al. 1996). Over the past century, climate change and human activities have significantly altered groundwater systems. Intensive exploitation of aquifers has resulted in a continuous decline of groundwater in some parts of the world such as northwest India, north China, and the central United States (Xia et al. 2007a, b; Wada et al. 2010; Pophare et al. 2014; Sarah et al. 2014; Scherberg et al. 2014). Overexploitation has raised concerns about resource sustainability and highlights the need for new approaches to groundwater use planning and management.

The Shule River basin is one of the three inland river basins in the Hexi Corridor in Northwest China. Groundwater plays an important role for irrigation and municipal use in this arid region. In the past 20 years a resettlement project of approximately 200,000 people, who mainly rely on agriculture, migrated into the area and has increased the stress on groundwater resources (Bao and Li 2006). Degradation of surface runoff has resulted in the disappearance of the terminal lake of Lop Nur (Xia et al. 2007a, b). Groundwater level declined from 1 to 5 m in the center of the Guazhou and Xihu district owing to groundwater withdrawal for agriculture. Desertification has also become a severe problem with the sand dune along the Shule River evolving from immobile to mobile dunes due to the degradation of vegetation cover (Ding et al. 2001). Given the region's agriculture and economic development, research should be carried out to quantify aquifers, recharge rates and natural water quality to ensure sustainable use of groundwater resources.

Conventional hydrogeology research methods such as water balance, the Darcian approach, lysimeters, water-table

fluctuations, and numerical simulation do not apply well in identifying groundwater availability in arid regions (Simmers 1997; Scanlon et al. 2002; Nimmo et al. 2005). In the past 60 years, the use of environmental tracers, including hydrogeochemical ions and environmental isotopes, has been used to examine water evolution through time providing insights that help researchers track hydrogeochemical characteristics of groundwater (Scanlon et al. 2002; Glynn and Plummer 2005; Liu and Yamanaka 2012). Major ions including Ca^{2+}, Mg^{2+}, Na^{+}, K^{+}, SO_4^{2-}, Cl^{-}, NO_3^{-} and alkalinity are used as natural tracers to identify water type and water–rock interactions (Ray and Mukherjee 2008; Mendizabal et al. 2011; Okkonen and Kløve 2012; Barberá and Andreo 2015). Based on oxygen and hydrogen isotopes of water, hydrogeology processes such as flow regimes and sources of recharge can be understood (Fontes 1980; Clark and Fritz 1997; Chen et al. 2011; Wang et al. 2013; Luoma et al. 2015). The radiocarbon date and concentration of $\delta^{13}C$ in dissolved inorganic carbon in groundwater can identify the residence time and infer the recharge information of a sampled groundwater (Münnich 1957; Ingerson and Pearson 1964; Tamers 1975; Mook 1976; Fontes and Garnier 1979; Landmeyer and Stone 1995; Geyh 2000; Han et al. 2014).

The Shule River basin has been the site of previous hydrogeochemical research. Qu and Yu (2007) investigated the conversion between different water bodies using major ions. Ma et al. (2013) dated confined groundwater as late Pleistocene in the western part of the river basin. Wang et al. (2005a, b) and Li et al. (2011) discussed the groundwater recharge source using stable isotopes in the northwest edge of the basin; however, a comprehensive study of geochemical indicators to understand regional groundwater dynamics is lacking. Groundwater study in relation to its chemical characteristics and processes that control groundwater quality has not been well defined. Additional areas lacking a clear understanding include groundwater recharge sources, recharge quantity, and timing and mechanisms of replenishment.

Through the investigation of groundwater geochemical processes and isotopic and radiocarbon distribution in aquifers, this study sought to pinpoint the source and characteristics of groundwater, and to determine the residence time and recharge rate of the groundwater. The results of this study will provide a better understanding of water resources in the Shule River basin and help the government develop suitable utilization strategies to manage the limited water resource.

Study area

The Shule River basin is located in the western part of Gansu province in Northwest China (Fig. 1a; bounding coordinates: 92°11′N–99°00′N and 38°00′E–42°48′E). The total area of this watershed is approximately 41,300 km^2 bound by the Qilian Paleozoic geosynclinal fold zone to the south and the Variscan fold belt (the Beishan Mountains) to the north. It shares boundaries with the Heihe River basin in the east, and spreads into Kumtag Desert in the west (Fig. 1b).

The river basin has three different geomorphological units: the Qilian Mountains in the south, the Beishan Mountains in the north and the plains between them. The southern Qilian Mountains consist of a series of east–west trending hills with elevations higher than 2,000 m above sea level (asl). The zones above 4,000 m asl are covered with snow and glaciers throughout the year. The glacier area and reserve volume are 850 km^2 and 4.6×10^{10} m^3, respectively. In the Shule River basin, almost all surface runoff originates from the high mountains. The river system is composed of the main channel of the Shule River and tributaries such as the Danghe River, Lucao River, Yulin River and other small temporary streams (Fig. 1b). The total volume of Shule River is about 16.3×10^8 m^3 $year^{-1}$. The annual precipitation is between 100 and 200 mm in the middle and high Qilian Mountains and reaches 600 mm in the glacier zone. The multiyear mean temperature is below 3.5 °C. The north Beishan Mountains range from 1,400–2,400 m in elevation and experience an extremely arid inland climate with high evaporation above 2,600 mm $year^{-1}$ (Chen and Qu 1992).

This study focuses mainly on the plains areas known as the Yumen-Tashi basin and the Guazhou basin that lie in a long belt from east to west between the two mountain ranges (Fig. 1c). The Yumen-Tashi basin ranges between 1,298 and 2,000 m in elevation from south to north. The climate is continental and the annual average temperature is 6.9 °C, the annual average precipitation is 63 mm and potential annual evaporation is 3,000 mm. Agriculture and petroleum extraction are the key economic activities. The Guazhou basin is situated in the downstream of Shule River basin with an average elevation of 1,500 m. The mean annual temperature is 8.8 °C ranging from −29.1 to 42.8 °C. The mean annual rainfall is approximately 45.7 mm with a potential annual evaporation of 3,140 mm (Chen and Qu 1992).

Geology and hydrogeology

The basic structural configuration of Shule River basin was created during a series of tectonic movements dating from the Mesozoic era. The middle depression occurred during the Triassic period and sunk quickly after the Yanshan Movement (Tapponnier et al. 1990; Meyer et al. 1998). During this period it received large amounts of Cenozoic deposition. Some structural hills such as the Nanjie Mountain, Beijie Mountain, and Hanxia Mountain were uplifted inside the depression zone cutting it into different parts. From the late Tertiary, especially from the end of the Pliocene and the beginning of the early Pleistocene, the Tibetan Plateau rose rapidly (Li et al.

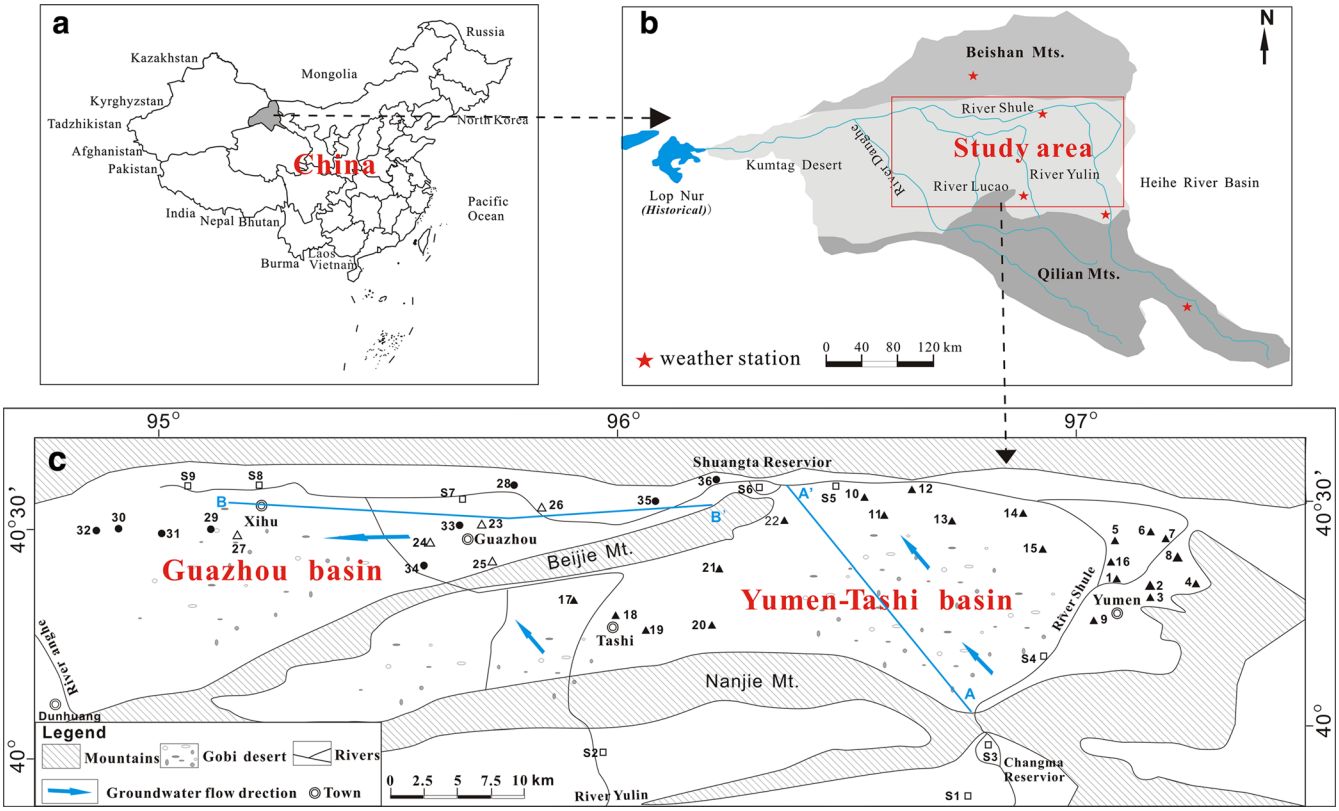

Fig. 1 **a–b** Study area and **c** sampling sites. The *solid triangles* represent sample points from Yumen-Tashi basin; *hollow triangles* and *solid circles* represent sample points from the Guazhou basin, shallow and deep, respectively; *hollow squares* represents surface-water sample points

1979). The intensive denudation and erosion led to significant transfer of clastic materials to the basin. For millions of years, the Shule River and its tributaries have transported cobbles and gravel into the depression. The main configurations of the depression are the diluvial fan, flood plain, alluvial delta, and the alluvial-lacustrine plain.

The aquifer system of the Yumen-Tashi basin includes the single-layer aquifer and the two-layer phreatic-confined aquifer. The single-layer aquifer is distributed on the Gobi zone of the Changma-Yulin proluvial fan and is made up of highly permeable cobble and gravel deposits. It has a thickness of generally 100–300 m, reaching 600 m in the piedmont of Qilian Mountains (Fig. 2). The water yield varies from south (east) to north (west). The well yield of Changma proluvial fan is more than 5,000 m^3 day^{-1}, and the groundwater level is 50–100 m below the surface. The well yield of Yulin proluvial fan is between 3,000 and 5,000 m^3 day^{-1}. In the north edge of the fan, the well yield declines to less than 1,000 m^3 day^{-1}, and the groundwater depth is 10–20 m. Rivers replenish the aquifer. The two-layer phreatic-confined aquifer is distributed on the fine soil plain, which spreads from the foreland of the northern Gobi area to the piedmont of the Beishan Mountains. The top layer of the aquifer is composed of interbedded sands and clays with a thickness less than 1 m. The water level varies from 1 to 5 m (Fig. 2) and well yield is below 1,000 m^3 day^{-1}. The thickness varies across the fine soil plain. The thicker areas are formed of cobbles and gravels and ranging between 20 and 80 m with a well yield of 5,000 m^3 day^{-1} (Gansu Geology Survey 1978). The thinner parts, comprised of sand and gravel, located in the northern basin, range between 3 and 10 m and the well yield is lower than 1,000 m^3 day^{-1}. In the fine soil plain, groundwater discharges as springs and is lost to evaporation and vegetation transpiration. The groundwater flow direction is very complex with a main flow from southeast to northwest (Gansu Geology Survey 1978).

The aquifer of the Guazhou basin transforms from a single-layer aquifer to multilayer phreatic-confined aquifers from east to west (Fig. 3). The single layer aquifer is mainly distributed in the piedmont of Beijie Mountain with a thickness of 70 m and is composed of gravel, pebbles, and sand. The water table is more than 10 m below the surface. The multilayer phreatic-confined aquifer is situated in the alluvial plain of the Shule River. The thickness is 25–30 m in the eastern plain, 30–40 m in middle of the Guazhou countryside, and below 20 m in the Xihu township. From east to west, the well yield decreases from about 4,000 to 700 m^3 day^{-1}. In the western part, the groundwater level of the aquifer is less than 5 m, and the hydraulic head of the confined water is 24 m

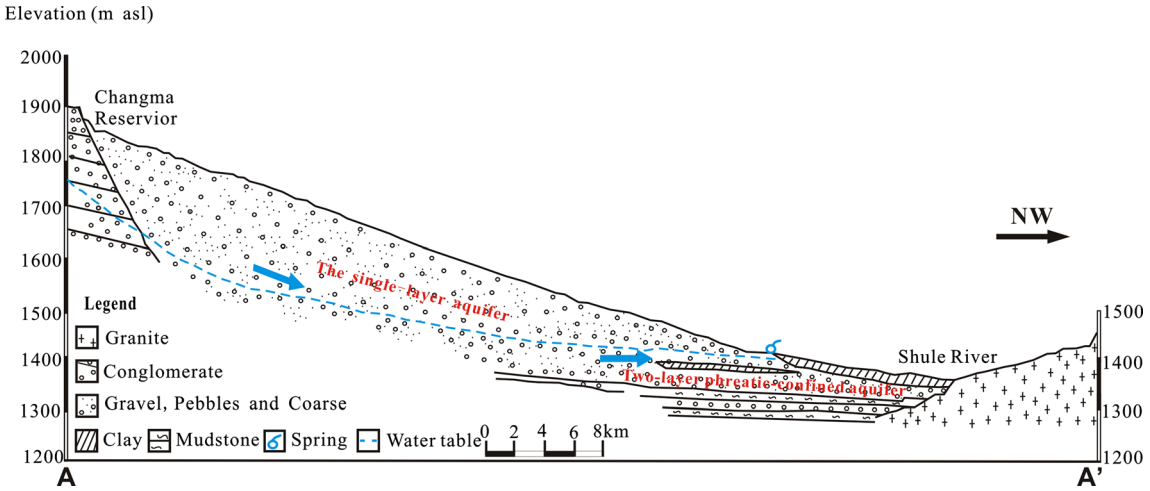

Fig. 2 Hydrogeologic cross-section along the transect *A–A′* in Fig. 1c

above the surface. The aquifer consists of gravel, sand, fine sand, and silty clay. The groundwater flows from east to west (Gansu Geology Survey 1978).

Materials and methods

Sampling and chemical analysis

Sampling was performed over four field trips from August 2011 to May 2013. Sampling sites include the oasis area, the Gobi area and the mountain range. Because the study area is huge geographically, fieldwork was costly and time consuming. Most samples were collected in 2011 but some remote sites were visited in 2012 and/or 2013. Some sites were sampled multiple times to examine the repeatability. Finally, a total of 36 groundwater samples and 9 surface-water samples were collected across the Shule River basin. Most of the groundwater samples were obtained from pumped wells during irrigation periods or from domestic water wells in communities. The surface-water samples were obtained from running water from upstream to downstream of rivers. Two primary reservoirs, the Changma reservoir and the Shuangta reservoir were sampled. The location of sample sites is shown in Fig. 1c. The basic data, including site information, elevation, and location (longitude and latitude) were recorded at each site. In addition, information on well depth, groundwater levels, and the structure of the boreholes was obtained from local water authority departments.

Temperature, specific electrical conductivity (SEC), pH, and total dissolved solids (TDS) were measured onsite using a sensION 156 portable multiparameter meter (Hach, Loveland, Colorado, USA). The total alkalinity (as HCO_3^-) was determined by a Model 16900 digital titrator (Hach) using bromocresol green-methyl red indicator, with a precision of ±1 % (SD) for values >100 digits. Thirty-milliliter samples for cation, anion, trace elements, and stable isotopic analyses were filtered in the field through 0.45-μm filters. Samples for cation and trace elements examination were acidified with concentrated HNO_3, producing a pH of around 1.5. All of the samples were stored in a chilling chamber with a temperature below 4 °C before measurement.

Major ions (Cl^-, SO_4^{2-}, NO_3^-, Na^+, K^+, Ca^{2+}, Mg^{2+}) and stable isotope ratios ($\delta^{18}O$, δ^2H) were determined at the Key Laboratory of Western China's Environmental System (Ministry of Education), Lanzhou University. Major ions were determined using an ICS-2500 ion chromatograph (Dionex,

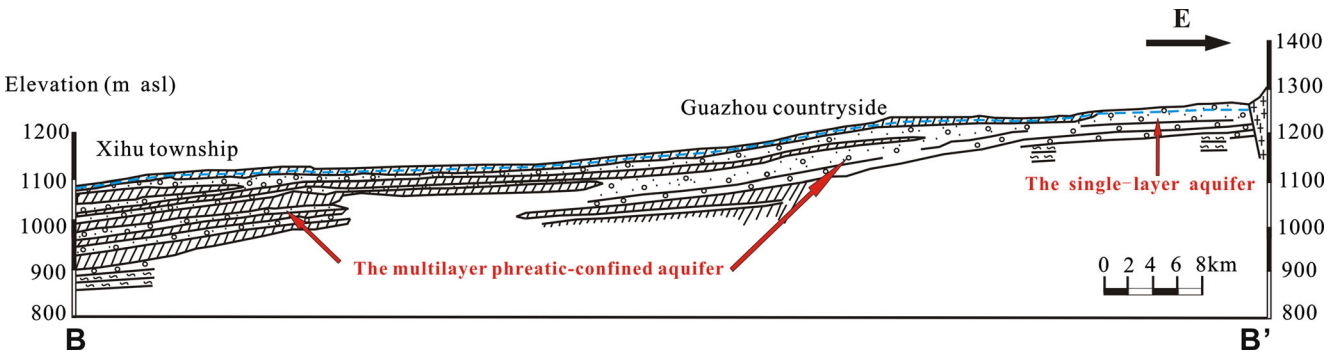

Fig. 3 Hydrogeologic cross-section along the transect *B′–B* in Fig. 1c, see the legend of Fig. 2 for description of features

Sunnyvale, California, USA) with an analytical precision of 3 % based on reproducibility of repeated analyses. All water chemistry results were within a 5 % ionic charge balance. Further examination of groundwater chemical evolution was based on the relationship of dissolved species in groundwater (Herczeg and Edmunds 2000). Stable isotopes ($\delta^{18}O$, $\delta^{2}H$) were measured using off-axis integrated-cavity-output laser spectroscopy (DLT-100, Los Gatos Research Inc.), following methods similar to that described in Lis et al. (2008). All measured values were reported according to Vienna Standard Mean Ocean Water (VSMOW). The precision was 0.2 ‰ for $\delta^{18}O$ and 1 ‰ for $\delta^{2}H$. The trace elements were carried out by ICP-MS (inductively coupled plasma mass spectrometry) at the Beijing Research Institute of Uranium Geology, China. Instrumental drift during ICP-MS analysis was corrected using In and Pt internal standards.

Samples for radiocarbon analysis were collected in 1-L Nalgene™ polyethylene bottles containing 5 ml of sodium hydroxide. The bottles were shipped to Beta Analytic Inc, in Miami, Florida, USA. The dissolved inorganic carbon (DIC) was reacted with strontium chloride ($SrCl_2$) to produce strontium carbonate ($SrCO_3$) precipitation. The precipitate was then acidified with H_3PO_4 to release CO_2 gas (Aggarwal et al. 2014). The CO_2 was subsequently reduced with H_2 to graphite over a Co catalyst (Vogel et al. 1987). Graphite targets were analyzed using accelerator mass spectrometry (AMS). The $\delta^{13}C$ was examined by isotope mass spectrography. ^{14}C results were reported as percent of the activity of modern carbon (PMC) and as the apparent radiocarbon age (BP), ^{13}C results were expressed as $\delta^{13}C$, relative to the Peedee belemnite international (VPDB) standard (Craig 1957). The essential step, using the radiocarbon value to date groundwater, is the estimation of the initial ^{14}C activity ($^{14}C_0$); however, it is difficult to get accurate $^{14}C_0$ because the groundwater undergoes many reactions during recharge and flow processes, and those affect the radiocarbon activity associated with the total dissolved inorganic carbon in groundwater. In this study, radiocarbon data were corrected using the Minqin model, which gives an upper limit of about 80 PMC for initial ^{14}C activity (Edmunds et al. 2006; Zhu et al. 2008; Ma et al. 2010). The groundwater age and its recharge status are represented in combination with the stable carbon isotope ratio ($\delta^{13}C$). In addition, ^{14}C age can be used to evaluate groundwater recharged rate (R) by Vogel's method (Vogel 1967). R is expressed as:

$$R = \frac{H\varepsilon}{xt}\left[x\ln\left(\frac{H}{H-z}\right) + x^{*}\right] \quad (1)$$

where H defines the total thickness of the aquifer and ε equals the mean aquifer porosity. The horizontal length of recharge area is x, and confined portion of the aquifer is x^{*}. z is sample depth below the water table. t is the age of a groundwater parcel at depth z.

Saturation index (SI)

The saturation index (SI) is a calculated number used to predict the stability of a specific mineral in a water system. SI is defined by the following equation (Lloyd and Heathcote 1985):

$$\mathrm{SI} = \log\left(\frac{\mathrm{IAP}}{K_S(T)}\right) \quad (2)$$

where IAP is the ion activity product of the solution, and $K_S(T)$ is the equilibrium constant of the reaction considered at temperature T.

For SI=0, water is in equilibrium with the mineral, for SI>0 water is super saturated and tends to precipitate the mineral, for SI <0 water is under-saturated and tends to dissolve the mineral. In this study, the PHREEQC program was used to calculate the SI for speciation (Parkhurst and Appelo 1999).

Hierarchical cluster analysis (HCA)

Cluster analysis is a multivariate statistical technique used to find groups of data (Bailey 1994). Hierarchical cluster analysis (HCA) is one cluster analysis technique and is often used for classification of hydrogeochemical data (Davis 1986; Schot and van der Wal 1992). In this study, the Euclidean distance was chosen as the distance measure and Ward's method (Ward 1963) was used to form clusters. Ward's method uses an analysis of variance approach to evaluate the distances between clusters to form smaller distinct clusters (StatSoft Inc 1995). The Euclidean distance (d_{ij}) between two samples of x_{it} and x_{jt} is defined as:

$$d_{ij} = \left[\sum_{t=1}^{p}\left(x_{it}-x_{jt}\right)^2\right]^{1/2}$$

where t defines each of the ions.

With HCA, a dendrogram is created whereby samples are linked into clusters on the x-axis and the linkage distances are plotted on the y-axis. Linkage distances between clusters illustrate relative similarities in the chemistry of the samples. A low distance indicates the two clusters are similar. A phenon line should be given across the dendrogram according to the researcher's judgment; thus, the number of clusters can be defined by moving the position of the phenon line up or down on the dendrogram (Güler et al. 2002), making HCA a semi-objective method. SPSS 20 for Windows (Bühl 2012) was used for the HCA in this study.

Results

The results of the chemical and stable isotope analyses of the Shule River basin were separated into three representative groups: the Yumen-Tashi groundwater, the shallow wells of the Guazhou basin with depth to 80 m, and the deep wells of the Guazhou basin.

Groundwater geochemical characteristics and hierarchical cluster analysis (HCA)

Basic physical information including well depth, temperature, pH and analytical chemical results of surface water and groundwater is presented in Table 1. The surface water from the upper reaches of Shule River had a TDS value of 247 mg L^{-1}, while the surface water from the upper reaches of Yulin River had a TDS value of 444 mg L^{-1}. The TDS value of surface water from the Shuangta reservoir was 292 and 358 mg L^{-1} from the Changma reservoir, and the TDS increased along the surface-water flow in the basin. The groundwater in the study area was generally fresh with TDS values between 255 and 2,560 mg L^{-1} (Table 1). In general, samples had neutral to slightly alkaline pH (6.8–8.3). The TDS of the Yumen-Tashi basin groundwater was between 255 and 1,340 mg L^{-1} with an average value of 594 mg L^{-1} (Table 1). In the eastern part of the Yumen-Tashi basin, the TDS of groundwater samples was around 500 mg L^{-1}, and the concentration of NO_3^- was relatively low with a mean value of 9.4 mg L^{-1}. Groundwater temperature was low, it was 4.4 and 5.2 °C in sample 4 and 5, respectively. In the middle section of the Yumen-Tashi basin, groundwater had low mineralization and ion concentrations. The concentration of NO_3^- was below 7.0 mg L^{-1} and Cl^- was generally below 63.0 mg L^{-1}. Groundwater from the western part of the Yumen-Tashi basin had elevated mineralization ranging from 816 to 1,340 mg L^{-1}. In the Guazhou basin, the TDS of all of the shallow groundwater increased from east to west along the direction of groundwater flow. The deep groundwater in the Guazhou basin had lower TDS than shallow groundwater (Table 1).

The results of the chemical analyses are illustrated in the Piper diagrams of Fig. 4. The surface water from the upper reaches of Shule River had a $CO_3^{2-}+HCO_3^-$ composition and the surface water from the upper reaches of Yulin River had a SO_4^{2-} composition. Most surface-water samples in the middle and lower reaches of the basin had SO_4^{2-} composition and the cation facies changed from Ca^{2+} to no-dominant class to $Na^+ + K^+$ (Fig. 4). Most of the groundwater in the Yumen-Tashi basin had a SO_4^{2-} composition. There was no obvious clustering of groundwater cations (Fig. 4). In the Guazhou basin, all of the shallow groundwater had SO_4^{2-} composition. The cation facies changed from a mixed composition to Na^+. The deep groundwater in the Guazhou basin had SO_4^{2-}–Na^+ composition (Fig. 4).

The dendrogram resulting from the HCA of the chemical data is shown in Fig. 5. In this study, nine variables including TDS, Cl^-, SO_4^{2-}, NO_3^-, HCO_3^-, Na^+, K^+, Ca^{2+}, Mg^{2+} were entered when doing the statistical analyses of HCA. Log transformation of data was applied to make the data into the normal distribution. To form geochemically distinct clusters, samples with a linkage distance less than 7 were grouped into together. The resulting four clusters are related by geographic location and well depth. Samples from C3 and C4 have lower distances indicating that these samples are geochemically similar. Most of these samples are from the Yumen-Tashi basin. C1 and C2, which consist of most of the samples from the Guazhou basin, are distinct from C3 and C4. Most samples collected from the eastern part of the Yumen-Tashi basin plot as one cluster (C3). Many samples from the middle section and western part of the Yumen-Tashi basin were linked in C4. C1 contains the majority of deep samples from the Guazhou basin.

Evolution of the groundwater chemistry

The SI values of the groundwater for halite, gypsum, celestite, strontianite, calcite, aragonite and dolomite were negative (Table 2), indicating groundwater is undersaturated with respect to these minerals. The mean SI values of the three kinds of carbonate are all below −1 (Table 2), indicating that the dissolution of carbonates is weak.

The SO_4^{2-} concentration increased with Cl^- (Fig. 6a), and the Na^+ and Cl^- were well correlated (R^2=0.90; Fig. 6b), illustrating that groundwater is undergoing evaporation to some extent and is influenced by dissolution of halite. However, most of the groundwater had Na/Cl milligram equivalent ratio ranges greater than 1 (Fig. 6b), suggesting that the presence of excess Na^+ and other possible minerals (such as Glauber's salt) may participate in chemistry balance of Na^+. The Na^+ and SO_4^{2-} concentrations are strongly correlated (R^2=0.88; Fig. 6c), and the SO_4^{2-} and Ca^{2+} were also positively correlated (Fig. 6d), indicating that potential dissolution of Glauber's salt and gypsum have provided excess SO_4^{2-} in the groundwater.

The concentration of Sr^{2+}in groundwater increased along the groundwater flow direction in the two basins—Fig. S1 of the electronic supplementary material (ESM)—and the Sr^{2+}/Ca^{2+} molar ratio increased (Fig. 6e). The behavior of Sr^{2+} in nature is similar to that of Ca^{2+} (Mg^{2+}), which combines with carbonate or sulfate. As discussed before, the dissolution of celestite provided Sr^{2+} in the groundwater. The Na^+/Ca^{2+} increased downstream (Fig. 6f). Abundance of Na^+ may result in cation exchange to release Na^+ at the expense of other cations in groundwater. This is confirmed by positive chloroalkaline indices (CAI 1 and CAI 2; Schoeller 1965), which indicate that cation exchange took place in the

Table 1 Basic physical and chemical data for groundwater and surface water samples in the Shule River basin

Sample No.	Location	Well depth(m)	Temp. (°C)	pH	TDS mg L^{-1}	Ca^{2+}	Mg^{2+}	Na^{+}	K^{+}	HCO_3^{-}	Cl^{-}	SO_4^{2-}	NO_3^{-}	Sr^{2+} (ug L^{-1})	δ^2H (‰)	$\delta^{18}O$ (‰)
Yumen-Tashi groundwater																
1	East	50	11.4	7.25	440	50.3	20.6	43.7	2.6	120	44.6	163.0	16.9	-	−60.1	−9.1
2	East	75	10.1	6.94	644	75.8	31.1	61.6	3.7	114	65.4	300.2	13.1	853	−61.3	−9.4
3	East	84	11.0	7.03	598	73.4	26.4	55.4	3.4	70	53.6	309.0	11.1	944	−61.5	−9.1
4	East	9	4.4	7.83	659	40.5	10.8	165.6	4.3	130	112.8	290.1	3.2	950	−68.0	−9.8
5	East	70	5.2	6.84	555	64.7	31.0	59.9	5.2	157	51.8	257.5	2.6	695	−61.5	−9.8
6	East	5	16.0	7.50	1,117	77.3	51.1	139.4	19.5	189	114.0	490.0	4.5	–	−57.1	−9.1
7	East	80	17.9	7.65	484	56.3	16.4	58.3	2.5	167	50.6	158.7	9.6	–	−61.6	−9.7
8	East	70	23.5	7.53	862	85.3	34.0	92.9	4.1	109	125.0	346.0	12.9	–	−59.1	−9.4
9	East	70	11.9	7.70	520	66.7	25.8	48.9	3.2	177	52.2	190.1	15.4	791	−59.8	−9.2
16	East	70	14.0	7.73	407	50.4	15.5	39.7	2.7	57	51.0	182.0	4.3	540	−60.3	−9.5
10	Middle	50	12.7	8.23	265	31.2	10.3	25.5	2.4	70	31.8	93.6	2.3	517	−60.0	−9.3
11	Middle	65	13.2	8.10	296	30.6	9.2	21.4	1.9	64	30.0	81.9	2.5	386	−57.6	−9.3
12	Middle	50	12.8	7.43	993	128.5	71.8	178.8	13.8	56	280.3	681.6	1.2	3,360	−53.8	−8.3
13	Middle	60	13.6	8.29	380	50.9	15.0	43.8	2.6	50	54.9	169.8	3.8	538	−57.6	−8.8
14	Middle	60	11.0	8.07	431	47.3	16.9	53.5	2.7	50	62.6	207.2	1.9	724	−62.4	−9.7
15	Middle	80	12.6	8.00	304	42.2	11.7	27.2	2.0	89	37.5	102.9	6.5	470	−61.4	−9.4
20	Middle	100	13.4	8.02	255	29.6	9.9	26.1	2.2	91	27.9	74.5	2.1	551	−64.5	−10.0
22	Middle	20	13.0	8.17	274	31.7	10.2	29.1	2.5	78	32.6	92.1	2.3	477	−62.7	−9.8
17	West	80	13.4	7.78	816	60.2	41.8	126.9	5.0	46	123.9	389.3	7.4	1,404	−74.4	−10.8
18	West	120	13.1	7.87	1,002	75.5	45.6	174.6	5.7	64	144.4	567.0	10.0	2,415	−70.5	−10.2
19	West	70	12.8	7.53	1,340	111.6	53.1	270.4	6.9	48	205.6	858.9	21.8	2,772	−67.5	−9.9
21	West	5	12.7	7.19	1,106	100.0	56.2	114.3	16.9	284	168.1	350.4	0.0	2,908	−62.7	−9.8
Mean.			11.7	7.70	594	62.7	27.9	84.5	5.3	104	87.3	288.9	7.1	1,183	−62.1	−9.5
Guazhou shallow groundwater																
23	Middle	50	13.2	6.92	1,337	114.7	54.7	224.1	9.2	76	267.0	665.7	18.4	1,678	−55.3	−8.4
24	Middle	70	14.8	7.28	2,560	216.5	114.1	444.0	17.9	67	545.5	1,349.2	22.4	4,831	−54.1	−7.7
25	Middle	40	15.3	7.64	1312	131.6	42.3	273.0	9.7	56	290.4	745.4	6.2	2,606	−59.3	−8.7
26	Middle	40	13.6	7.24	668	60.0	29.2	94.6	7.0	45	106.8	337.9	7.5	1,386	−53.6	−7.8
27	West	60	14.5	7.26	2,230	153.6	48.0	560.6	27.3	124	510.3	1,151.0	24.2	–	−66.6	−9.1
Mean.			14.3	7.27	1,621	135.3	57.7	319.3	14.2	74	344.0	849.8	15.7	2,625	−57.8	−8.3
Guazhou deep groundwater																
35	East	100	12.5	8.07	928	100.6	39.2	139.3	6.6	136	154.3	464.0	5.2	1,278	−53.1	−8.0
36	East	120	12.5	7.99	696	85.5	28.3	95.0	6.9	50	101.5	385.5	6.0	1,087	−52.5	−8.4
28	Middle	120	13.7	7.72	1,277	130.8	8.5	319.1	4.5	55	404.1	562.0	14.1	1,947	−65.6	−9.4
33	Middle	120	13.9	7.31	524	35.8	14.4	105.0	5.3	123	80.7	209.1	2.0	581	−60.3	−8.9
34	Middle	200	14.6	7.85	757	67.5	25.5	144.8	6.8	45	131.1	361.1	1.7	856	−61.0	−9.5
29	West	120	17.3	7.69	919	73.2	18.6	199.8	3.2	78	167.0	437.1	12.2	–	−69.5	−9.7
30	West	90	15.2	7.56	1,065	91.5	24.6	223.0	11.4	72	183.6	587.1	11.8	–	−70.9	−9.7
31	West	81	14.6	7.74	1,050	89.4	24.5	220.8	10.5	70	179.4	571.9	10.1	–	−71.0	−9.5
32	West	90	14.0	7.81	1,203	98.8	28.0	260.6	6.5	74	193.0	657.1	9.8	–	−70.7	−9.6
Mean.			14.3	7.75	935	85.9	23.5	189.7	6.9	78	177.2	470.5	8.1	1,150	−63.8	−9.1
Surface water																
s1	Upstream	–	21.8	8.41	247	36.4	9.6	13.5	1.3	136	8.8	53.9	3.1	–	−72.5	−10.9
s2	Upstream	–	19.0	8.17	444	48.7	20.0	42.6	3.0	117	38.4	172.2	2.0	771	−75.4	−11.9
s3	Changma reservoir	–	6.1	8.31	358	62.9	17.3	29.7	1.9	193	30.8	118.3	2.9	426	−60.9	−8.7
s4	Midstream	–	–	7.98	365	63.0	17.5	29.7	2.0	195	30.8	120.2	2.9	–	−61.7	−9.1
s5	Midstream	–	22.8	8.37	421	55.0	16.0	46.5	3.6	45	61.6	213.0	1.7	–	−53.3	−8.4

Table 1 (continued)

Sample No.	Location	Well depth(m)	Temp. (°C)	pH	TDS mg L^{-1}	Ca^{2+}	Mg^{2+}	Na^{+}	K^{+}	HCO_3^{-}	Cl^{-}	SO_4^{2-}	NO_3^{-}	Sr^{2+} (ug L^{-1})	δ^2H (‰)	$\delta^{18}O$ (‰)
s6	Shuangta reservoir	–	25.7	8.45	292	42.5	9.9	27.8	2.5	63	34.3	127.2	1.7	–	−51.7	−8.3
s7	Downstream	–	25.7	8.43	288	41.6	9.7	27.8	2.3	66	34.3	126.9	1.8	–	−51.1	−8.3
s8	Downstream	–	27.3	8.44	568	55.7	18.5	115.6	4.2	144	105.1	235.3	1.9	–	−49.0	−7.6
s9	Downstream	–	22.2	8.94	1,672	108.8	37.3	372.7	7.6	73	431.3	652.6	11.1	–	−28.3	−2.4

groundwater. There were no trends in HCO_3^{-} vs (Ca^{2+} + Mg^{2+}) in groundwater, and there was a deficiency in HCO_3^{-} relative to (Ca^{2+} + Mg^{2+}; Fig. 6h), indicating the reaction of the carbonate is negligible.

Groundwater stable isotopes

A local meteoric water line (LMWL) was determined by Zhao et al. (2011) using isotopes in precipitation in 2008 and 2009 at the Yeniugou National Meteorological station some 200 km E of Shule River basin; this is a representative position in the Qilian Mountains. Although this is not a long time-series dataset, it is valuable for use in the present study. In Northwest China, water mainly originates from the high Qilian Mountains and as a result, local water lines from the area can provide basic information (He et al. 2012). The defined line is expressed as $\delta^2H=7.647\ \delta^{18}O+12.396$ (R^2= 0.989, n=99; Zhao et al. 2011). Figure 7 shows the stable isotope data for surface water and groundwater samples in Shule River basin within the LMWL and local surface-water evaporation line.

The surface water showed a high degree of variability in $\delta^{18}O$ and δ^2H ranging from −11.9 to −2.4 ‰, and −75.4 to −28.3 ‰, respectively (Table 1). The isotopic ratios of surface water have a slope of 5.07 and an intercept of −11.1 ‰ on the LMWL (Fig. 7a). This intercept value is close to the average value of the headwaters of Shule River and Yulin River. According to the mean altitude effect of about −0.18 ‰/100 m (Wang et al. 2009), the surface water consisted of glacial and precipitation inputs at elevations around 4,500 m. The isotopic compositions of the samples from Shuangta reservoir and running water of the Guazhou basin converged on the local meteoric water line with a mean value of −8.3 ‰ $\delta^{18}O$ and −53.8 ‰ δ^2H (Fig. 7a).

The groundwater of Shule River basin had $\delta^{18}O$ values ranging from −10.8 to −7.7 ‰ and δ^2H values ranging from −74.4 to −53.1 ‰ (Table 1). The plots of groundwater samples form a line distributed along the LMWL, and were much more depleted than the values of local rainfall (−6.5 ‰ $\delta^{18}O$, −44 ‰ $\delta^{18}O$; Ma et al. 2010). In the Yumen-Tashi basin, groundwater $\delta^{18}O$ values ranged between −8.3 and −10.8 ‰, and the δ^2H values ranged between −53.8 and

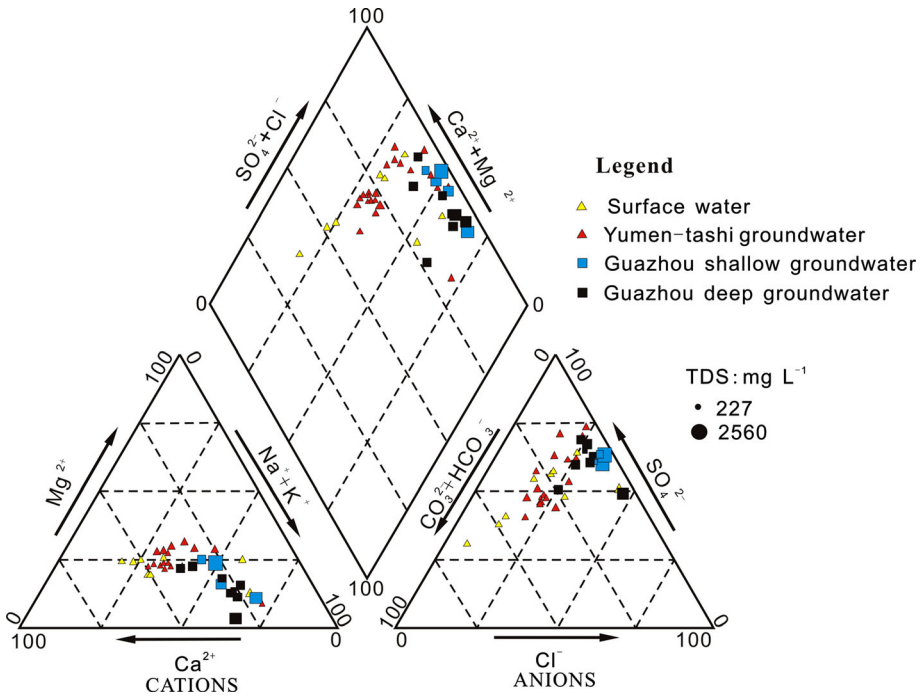

Fig. 4 Piper trilinear plots for the chemical compositions of the surface water and groundwater

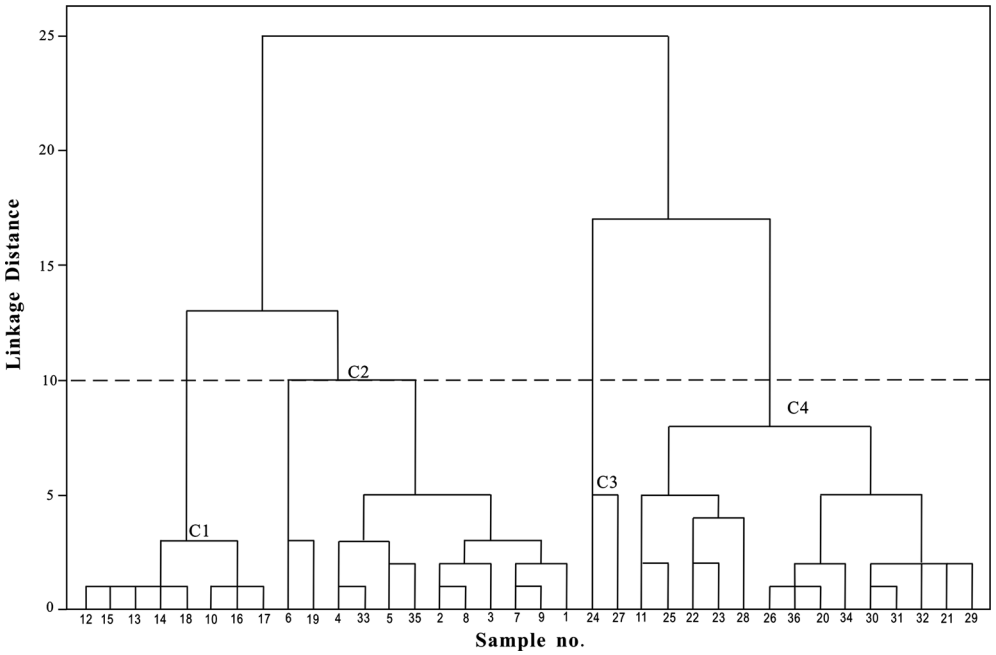

Fig. 5 Dendrogram of groundwater samples

−74.4 ‰ (Table 1). Most samples show a linear trend close to the LMWL. The $\delta^{18}O$ values of groundwater in the east of the basin ranged from −9.1 to 9.8 ‰, which was close to the value of surface water (sample s4). Groundwater samples in the west were depleted in isotopes. In the middle section, samples around the Changma proluvial fan had similar values, which is consistent with the hydrogeologic condition that groundwater may flow through palaeo-river channels of Shule River. The shallow groundwater in the fine soil plain of the Guazhou basin was enriched with heavy isotopes, and all of the values plotted below the LMWL (Fig. 7). In contrast, the deep groundwater of the Guazhou basin was depleted of heavy isotopes. The $\delta^{18}O$ values ranged from −9.7 to −8.0 ‰ and the $\delta^{2}H$ values ranged from −71.0 to −52.5 ‰ (Table 1). The mean values of $\delta^{18}O$ and $\delta^{2}H$ were −9.1 and −63.8 ‰, respectively (Table 1). In particular, groundwater in wells 29 and 30 was the most depleted in heavy isotopes. Two deep samples (samples 35 and 36) in the east of the basin show similar isotopic values with the surface water (sample s5).

Table 2 Mean and range for the saturation indices (SI) for commonly occurring minerals. Values were calculated using the PHREEQC software

Phase	SI		
	Min	Max	Mean
Aragonite	−1.53	−0.51	−1.16
Calcite	−1.38	−0.36	−1.01
Dolomite	−2.94	−0.63	−2.15
Celestite	−3.2	−1.35	−2.40
Gypsum	−3.08	−1.42	−2.25
Halite	−7.74	−5.18	−6.57
Strontianite	−2.83	−1.45	−2.41

Radiocarbon geochemistry and groundwater age

The ^{14}C results for 10 deep groundwater samples ranged from 3.84 to 79.59 PMC with a corresponding residence time from several decades to tens of thousands of years. The $\delta^{13}C$ values lay between −1.9 and −16.2 ‰ (Table 3). The radiocarbon data showed a progressive decrease in activity along the groundwater flow direction in both the Yumen-Tashi and Guazhou basins (Fig. S2 of the ESM). The $\delta^{13}C$ values exhibit the opposite trend along the groundwater flow direction, with the heaviest values found in the deep groundwater of the lower reaches of the Guazhou basin (Fig. S2 of the ESM). The groundwater samples are generally undersaturated with respect to carbonate minerals (Table 2). Carbonate minerals are rare or absent in these aquifers (Gansu Geology Survey 1978). It is probable that the radiocarbon evolution was controlled by the closed system decay and $\delta^{13}C$ values observed were derived from dilution of soil CO_2 in the recharge areas and its reactions with silicate minerals.

In the Yumen-Tashi basin the ^{14}C concentrations decreased from 69.01 to 33.15 PMC from east to west and the $\delta^{13}C$ values were between −4.5 and −16.2 ‰ (Table 3). In the east of the Yumen-Tashi basin, the ^{14}C was high and close to the assumed value of 80 PMC and the $\delta^{13}C$ value was −7.3 ‰ similar to atmospheric concentrations (Keeling et al. 2005). This is consistent with the recharge condition of this region. Surface water quickly enters into the underground through the sandy gravel. Because of the extremely arid climate, this area lacks vegetation and the activity of soil microorganisms is weak. The $\delta^{13}C$ values reveal the characteristics of dissolved carbon from the atmospheric. The radiocarbon composition and $\delta^{13}C$ of groundwater in the middle section of Yumen-

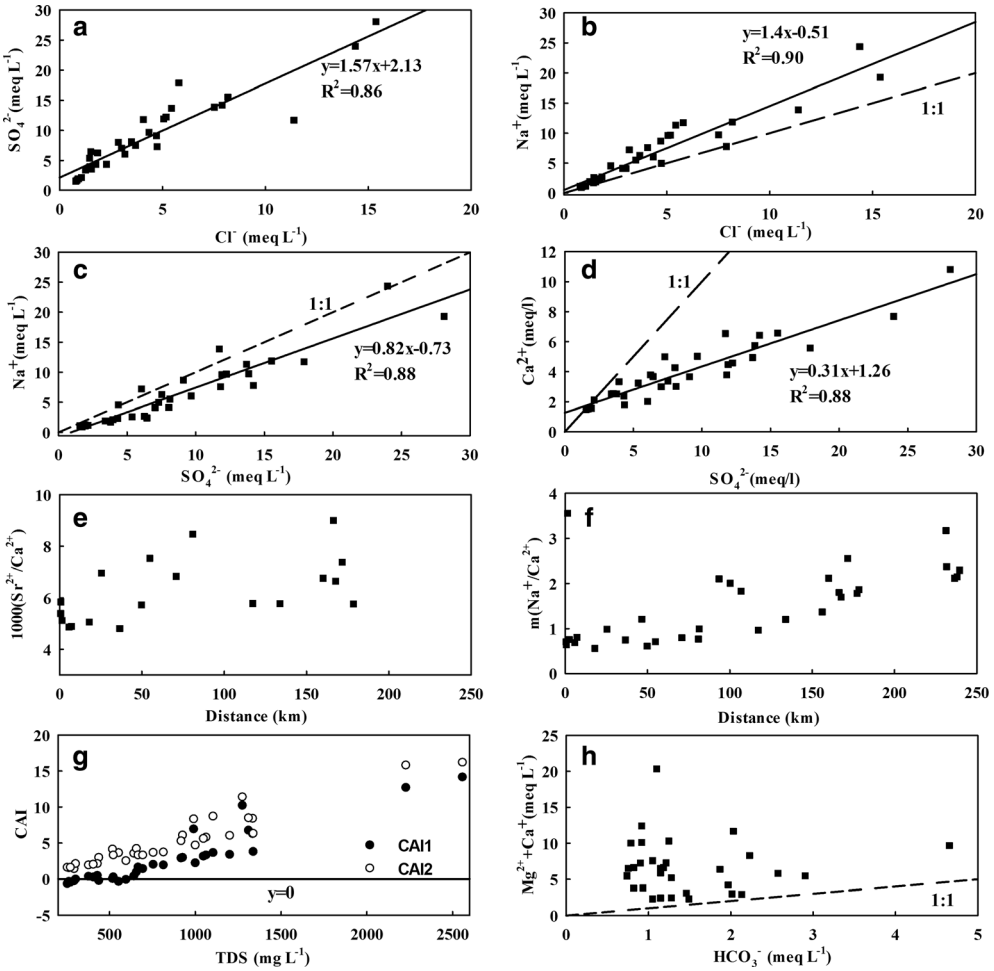

Fig. 6 Correlations between molar ratios and molar ratios and distance from the groundwater samples in the study area. Parameters with an "m" prefix, such as m (Na^+/Ca^{2+}), represent milligram equivalent ratios. The *dashed lines* represent the theoretical dissolution curves for **b** halite, **c** Glauber's salt, **d** gypsum. *Solid lines* (**b**–**d**) represent significant regression results. *Distance* is the length along the transects of A–A′ or B′–B (see Fig. 1). In this study, the sites were projected onto the transects A–A′ or B′–B in the two basins, and *Distance* indicates the length from point A (or B′) to the subpoint. For samples of Yumen-Tashi basin, the distance is the length between point A and the subpoint; for samples of the Guazhou basin, the distance is the length between point B′ and the subpoint plus length of A–A′

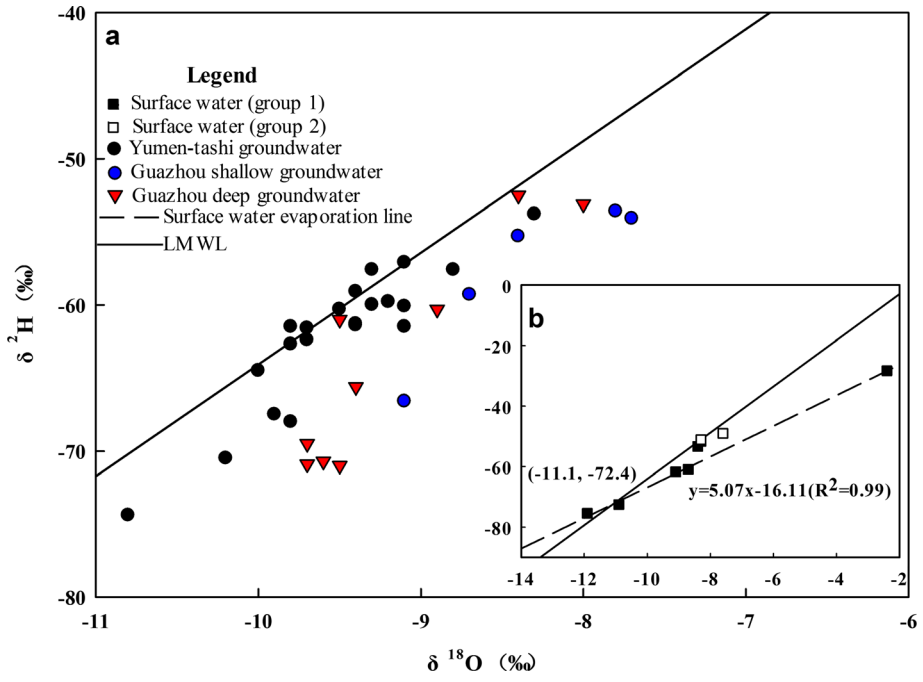

Fig. 7 Stable isotope ratios in Shule River basin, **a** stable isotope plot of the groundwater, and **b** stable isotope plot of the surface water, with the surface-water evaporation line and local meteoric water line (*LMWL*)

Table 3 Radiocarbon results and corrected ^{14}C age for deep groundwater samples

Sample No.	^{14}C (PMC)	$\delta^{13}C$ (‰ PDB)	Apparent ^{14}C age (years)	Minqin model (years)
9	69.01	−7.3	2,980 ±30	1,222
11	38.78	−16.2	7,610 ±40	5,986
14	53.73	−4.5	4,990 ±30	3,291
15	42.311	−5.4	6,910±40	5,266
17	33.15	−1.9	8,870 ±40	7,283
29	3.84	−3.6	26,180±120	25,103
33	50.78	−5.19	5,445±35	3,758
34	41.16	−12.8	7,130 ±40	5,494
35	75.29	−8.1	2,280 ±30	502
36	79.59	−6.2	1,835±35	42

Tashi basin showed a different pattern. Some samples were depleted in $\delta^{13}C$ but had medium ^{14}C concentration. Lighter ^{13}C values indicated the direct dissolution of soil carbon dioxide when water passes through the vadose soil zone. These areas have widespread agriculture and the vegetation is predominantly C_3 species, which would give rise to a soil CO_2-$\delta^{13}C$ of around −23 ‰ (Wang et al. 2005a, b). The heaviest values expected for total dissolved inorganic carbon (TDIC) were around −15 ‰ $\delta^{13}C$, after allowing for isotopic fractionation at the near neutral pH. Some of the samples from this zone had high concentrations of $\delta^{13}C$ with a mean value of −5.0 ‰, which is further indication that the groundwater may derive from soil CO_2 reactions with silicate minerals. The groundwater age was between 3,000 and 6,000 years old (Table 3).

In the Guazhou, basin the $\delta^{13}C$ and groundwater age had the same trend with the Yumen-Tashi basin (Fig. 8; Fig. S2 of the ESM). However, the deep groundwater in lower reaches of the Guazhou basin was very old with a calculated age around 25,000 years BP.

Discussion

The Shule River basin in Northwest China is facing increasing stress on groundwater resources. The Quaternary aquifers are closely connected with streams originating from Qilian Mountains and river systems across the river basin. Groundwater around the Changma proluvial fan of the Yumen-Tashi basin has similar isotopic values to the rivers

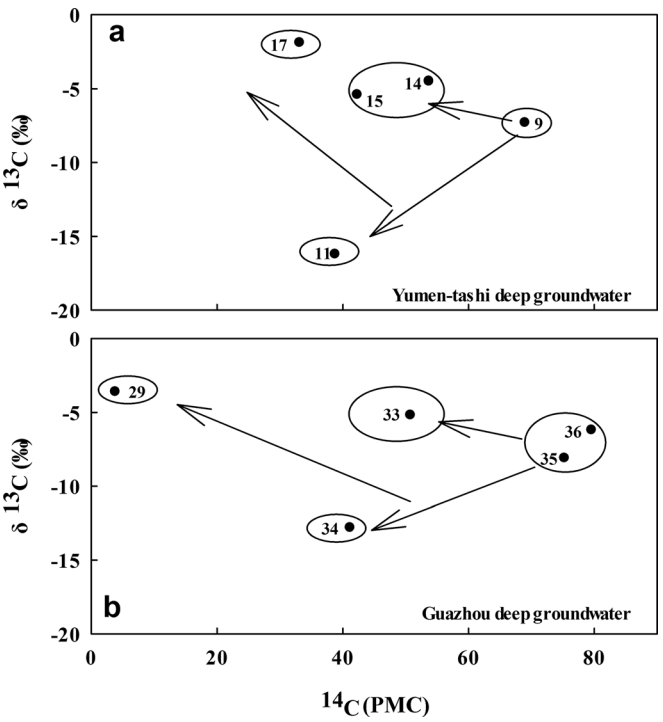

Fig. 8 Plot of $\delta^{13}C$ against ^{14}C for deep groundwater from the study area: **a** Yumen-Tashi basin and **b** Guazhou basin

Table 4 Recharge rate estimated from ^{14}C ages

Sample No.	^{14}C age (years)	x [km]	x^* [km]	z [km]	R [mm/year]
9	1,222	25	10	60	23
11	5,986	40	12	55	4
14	3,291	48	13	50	6
15	5,266	41	4	70	7
17	7,283	46	31	70	6
29	25,103	15	93	50	4
33	3,758	15	35	50	13
35	502	15	4	30	23

suggesting that the subsurface flow through the paleochannels of Shule River supplies the aquifer. This is also confirmed by the lower rates of mineralization and ion concentrations in groundwater. The low concentration of Cl^- and NO_3^- indicates infiltration from surface waters without many anthropogenic inputs. Fractures, created through tectonic movement, may control the flow into the east Yumen-Tashi basin (Gansu Geology Survey 1978). The water appears to flow from the mountains through the fractures in a short time, maintaining low temperatures. The high radiocarbon activity of groundwater is consistent with the active recharge in the area. These findings are consistent with observations from the nearby Badain Jaran Desert where water from Yabulai Mountain is transported to the plains areas through fractures (Gates et al. 2008a). Deep groundwater in the eastern part of the Guazhou basin had similar stable isotope characteristics to surface water, suggesting a close connection between them. The groundwater residence time ranged from decades to hundreds of years in this area, also providing evidence of active recharge in the aquifer. The shallow groundwater in the fine soil plain of the Guazhou basin was enriched with heavy isotopes and plotted below the LMWL. The TDS values of groundwater increased from east to west along the groundwater flow, revealing that evaporation and return of irrigation water had occurred, which changed the isotopic and chemical feature of the recharged water. Strong linear relationships between Cl^- and Na^+, and between Cl^- and SO_4^{2-}, also largely indicate that evaporation is the primary control on groundwater hydrogeochemistry and discharge in this area. This is a typical phenomenon in arid areas, where water can be lost by evaporation from the unsaturated zone or from the water table (Hchaichi et al. 2014). It has been found that river and irrigation infiltration to the shallow and some deep aquifers in the piedmont fan can provide important water resources to Northwest China (Chen et al. 2006; Zhu et al. 2008; Ma et al. 2013). However, the river that flows into Yumen-Tashi basin has been controlled by the Changma reservoir since it was built in 2003. Today, significant extraction from channels in the Yumen basin has greatly reduced the runoff. The proportion of recharge from surface runoff is decreasing. In 2000, 74.5 % of the groundwater recharge in the upper part of the Yumen-Tashi basin was from river infiltration, and by 2008 that percentage was down to 38.7 %. The water table showed a 0.15 m rate of decrease each year from 2000 to 2010 in the piedmont of the proluvial fan (Huang and Wang 2010).

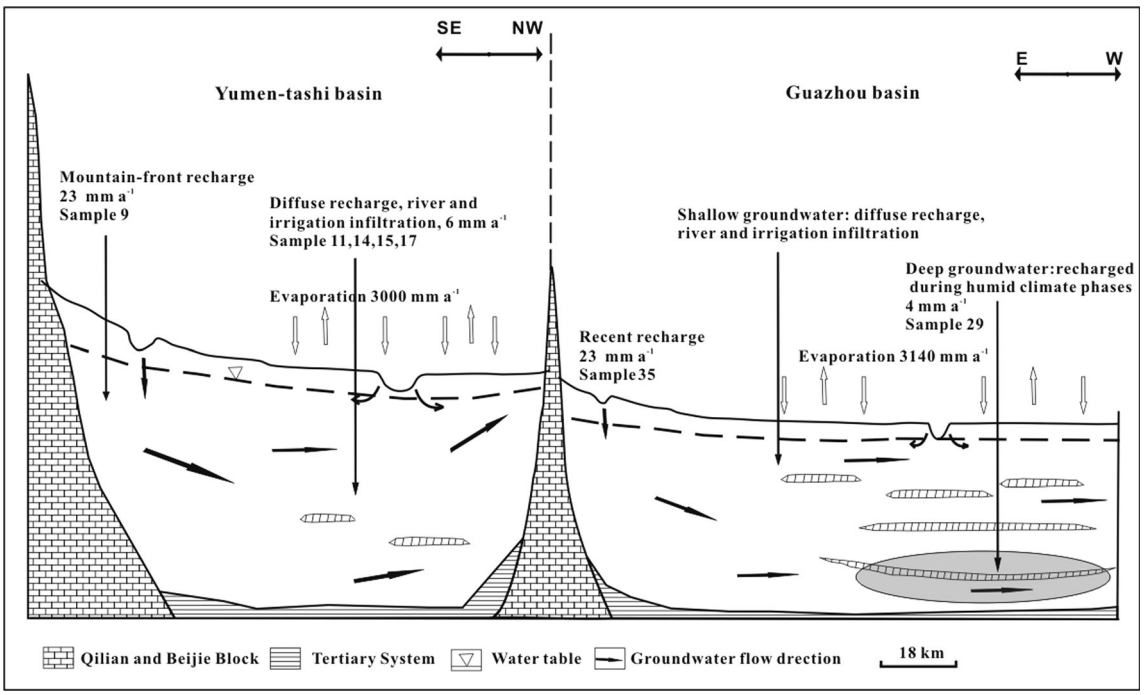

Fig. 9 Conceptual recharge model of the Shule River basin

Diffuse recharge to shallow groundwater has been shown to be minimal. The stable isotopes ($\delta^{18}O$ and $\delta^{2}H$) provide a distinction between the reference data for the modern rainfall (−6.5 ‰ $\delta^{18}O$, −44 ‰ $\delta^{2}H$; Ma et al. 2010) and groundwater of the study area (with average values of −9.3 ‰ $\delta^{18}O$ and −61.9 ‰ $\delta^{2}H$), illustrating the groundwater has been isolated from diffuse recharge. In arid regions, the diffuse recharge rate is limited owning to low precipitation and high evaporation as well as a thick vadose zone. Studies of the unsaturated zone in the Badain Jaran Desert and Tengger Desert confirm small amounts of direct recharge (Ma and Edmunds 2006; Gates et al. 2008b; Ma et al. 2009). Huang et al. (2013) reported that rainfall would take decades to hundreds of years to reach the water table in the Loess Plateau of China.

The stable isotope content for most of the deep groundwater samples was depleted. The age of deep groundwater was between 3,000 and 25,000 years BP. It is obvious that the groundwater contains a paleo-component from cooler hydrological eras and has been isolated from modern recharge for thousands of years. According to the local relationship between the temperature and $\delta^{18}O$ of rainfall (Liu et al. 2008), the calculated recharge temperature of the most depleted groundwater in the Guazhou basin was about 6.1 °C, which is 2.7 °C cooler than the modern mean annual air temperature of this area. This is consistent with the palaeoclimatic record of this region. A wetter mid-Holocene characterized by high precipitation, lush vegetation cover and high water levels of lakes was documented for lake sediments in central Asia (Chen et al. 2008). No samples from the early Holocene were found, which could be the result of an almost complete cessation of groundwater recharge at that time. During the early Holocene, conditions were dry in Central Asia and infiltration may have been reduced or even interrupted. These gaps in time have been identified in other aquifers around the world (Beyerle et al. 1998; Gasse 2000).

The groundwater flow velocity can be estimated using the difference in radiocarbon dates and positions between the two groundwater samples: sample 29 (age 25,103 years) is about 53 km further along the flow path from sample 33 (age 3,758 years), indicating an approximate flow velocity of 2.48 m $year^{-1}$. This result is concordant with that calculated based on the Darcy's law (Darcy 1856). Assuming a porosity of 0.20, saturated hydraulic conductivity of 3.0 m day^{-1}, and a hydraulic gradient of 5.2×10^{-4}, the average flow velocity of the deep groundwater is 2.85 m $year^{-1}$. Using radiocarbon dating and Vogel's method (Vogel 1967), and assuming a porosity of 0.20, other input data (including the thickness of the aquifer, horizontal length of recharge area, confined portion of the aquifer and sample depth presented in Table 4), the groundwater recharge rate was estimated to be between 4 and 23 mm $year^{-1}$ (Table 4). This indicates that groundwater flow is relatively slow and water resources sustained by this flow are essentially non-renewable in the aquifer.

Based on the aforementioned findings, a conceptual recharge model of the Shule River basin is proposed (Fig. 9). The humid climate of the late Pleistocene and middle Holocene probably led to replenishment by rainfall through mountain-front recharge and direct diffusive recharge. At present, groundwater recharge is decreasing due to aridification and human activities. The arid climate of the area is strongly controlled by westerlies (Dando 2005) and modern diffuse infiltration provides negligible recharge to the shallow aquifer. Most recharge originates from the Qilian Mountains where there is more precipitation and meltwater. Irrigation returns and surface-water infiltration are the recharge sources for the shallow groundwater in the fine soil plain. The deep aquifer of the piedmont has been recharged through a number of mechanisms, including lateral flow from the piedmont and modern-water direct vertical infiltration from river channels in the upper part of each basin. Groundwater flows towards the discharge zones from SE to NW (or W) in the Yumen-Tashi basin and from E to W in the Guazhou basin. The deep groundwater in the middle and lower reaches of the basins has a residence time of thousands of years, as early as the late Pleistocene and the recharge rate and groundwater flow velocity are slow. The aquifer is principally maintained by palaeowater and has no genetic relationship with modern recharge.

Conclusions

Chemical and isotopic tracers were used to characterize groundwater evolution and recharge mechanisms in the Shule River basin. The findings suggest that:

1. The groundwater in the study area was generally fresh with average TDS values increasing downstream. The groundwater ionic composition was dominated by SO_4^{2-}. The linear relationships between Na^+ and Cl^-, Na^+ and SO_4^{2-}, and Ca^{2+} and SO_4^{2-} confirm that dissolution of halite, Glauber's salt and gypsum control the concentrations of these ions. In addition, the dissolution of celestite and reverse ionic exchange were widely occurring in groundwater.
2. Modern recharge occurs mainly in the fine soil plain and in the piedmont of Qilian Mountains by a number of mechanisms, including direct vertical infiltration from river channels and irrigation returns, as well as small amounts from leakages through fractures.
3. Stable isotope and radiocarbon data suggest that the deep groundwater in the middle and lower reaches was recharged during the late Pleistocene to middle Holocene when rainfall was more abundant. Groundwater flow and recharge rates are relatively slow and the water resources are essentially non-renewable.

These results have important implications for groundwater management in Shule River basin. Groundwater in the Shule River basin has undergone different recharge phases from the late Pleistocene to Holocene, and modern recharge appears to be decreasing. The exploitation of fossil groundwater in this area is unsustainable, as moisture transport patterns are significantly different from the past. A water conservation strategy and changes to agricultural practices are urgently needed across the region to conserve groundwater.

Acknowledgements The research is supported by the National Science Foundation of China (Nos. 41402200, 41271039) and the Fundamental Research Funds for the Central Universities of Lanzhou University. We thank Mrs. Jingfang Wang and Mrs. Yanhui Pan in Lanzhou University and Dr. Darden Hood in the Beta Analytic Inc. for assistance in the laboratory analysis. We would also like to thank Alison Beamish at the University of British Columbia for her assistance with English language and grammatical editing of the manuscript.

References

Aggarwal PK, Araguas-Araguas L, Choudhry M, Duren MV, Froehlich K (2014) Lower groundwater ^{14}C age by atmospheric CO_2 uptake during sampling and analysis. Groundwater 52(1):20–24

Bailey K (1994) Numerical taxonomy and cluster analysis. Typol Taxonom 34:24

Bao W, Li J (2006) The study of the ecology effect of Shule River basin resettlement-cum-irrigation development project (in Chinese). Soil Water Conserv Sci Technol 6:4–6

Barberá JA, Andreo B (2015) Hydrogeological processes in a fluviokarstic area inferred from the analysis of natural hydrogeochemical tracers: the case study of eastern Serranía de Ronda (S Spain). J Hydrol 523:500–514

Beyerle U, Purtschert R, Aeschbach-Hertig W, Imboden DM, Loosli HH, Wieler R, Kipfer R (1998) Climate and groundwater recharge during the last glaciation in an ice-covered region. Sci Rep 282:731–734

Bühl A (2012) SPSS 20: Einführung in die moderne Datenanalyse [Introduction to modern data analysis]. Pearson, London

Chen LH, Qu YG (1992) Rational development and use of land resources in Hexi region (in Chinese). Science Press, Beijing, pp 65–100

Chen ZY, Nie ZL, Zhang GH, Wan L, Shen JM (2006) Environmental isotopic study on the recharge and residence time of groundwater in the Heihe River Basin, northwestern China. Hydrogeol J 14:1635–1651

Chen FH, Yu ZC, Yang ML, Ito E, Wang SM, Madsen DB, Huang XZ, Zhao Y, Sato T, Birks JB, Boomer I, Chen JH, An CB, Wünnemann B (2008) Holocene moisture evolution in arid central Asia and its out-of-phase relationship with Asian monsoon history. Quat Sci Rev 27(3):351–364

Chen ZY, Wei W, Liu J, Wang Y, Chen J (2011) Identifying the recharge sources and age of groundwater in the Songnen Plain (Northeast China) using environmental isotopes. Hydrogeol J19:163–176

Clark ID, Fritz P (1997) Environmental isotopes in hydrogeology. Lewis, New York, 328 pp

Clarke R, Lawrence A, Foster S (1996) Groundwater: a threatened resource. United Nations Environment Programme Environment Library No. 15, UNEP, Nairobi, Kenya

Craig H (1957) Isotope standards for carbon and oxygen and correction factors for mass spectrometric analysis of carbon dioxide. Geochim Cosmochim Acta 12:133–149

Dando WA (2005) Asia: climates of Siberia, central and East Asia. In: Oliver JE (ed) Encyclopedia of world climatology. Springer, Dordrecht, The Netherlands, pp 102–114

Darcy H (1856) Les fontaines publiques de la Ville de Dijon [The public fountains of the city of Dijon]. Dalmont, Paris

Davis JC (1986) Statistics and data analysis in geology. Wiley, New York

Ding H, Zhao C, Huang X (2001) The ecological environment and desertification in the Shule River basin (in Chinese). Arid Zone Res 18:5–10

Edmunds WM, Ma JZ, Aeschbach-Hertig W, Kipfer R, Darbyshire F (2006) Groundwater recharge history and hydrogeochemical evolution in the Minqin basin, North West China. Appl Geochem 21:2148–2170

Fontes JC (1980) Environmental isotopes in ground water hydrology. In: Fritz P, Fontes JC (eds) Handbook of environmental isotope geochemistry, vol 1. Elsevier, Amsterdam, pp 75–140

Fontes JC, Garnier JM (1979) Determination of the initial ^{14}C activity of the total dissolved carbon: a review of the existing models and a new approach. Water Resour Res 15:399–413

Gansu Geology Survey (1978) The report and map for hydrogeological survey in the Shula River basin (1: 200 000). Gansu Science and Technology Press, Lanzhou, China

Gasse F (2000) Hydrological changes in the African tropics since the last glacial maximum. Quat Sci Rev 19(1):189–211

Gates JB, Edmunds WM, Darling WG, Ma J, Pang Z, Young AA (2008a) Conceptual model of recharge to southeastern Badain Jaran Desert groundwater and lakes from environmental tracers. Appl Geochem 23:3519–3534

Gates JB, Edmunds WM, Ma J, Scanlon BR (2008b) Estimating groundwater recharge in a cold desert environment in northern China using chloride. Hydrogeol J 16:893–910

Geyh MA (2000) An overview of ^{14}C analysis in the study of groundwater. Radiocarbon 42:99–114

Glynn PD, Plummer LN (2005) Geochemistry and the understanding of groundwater systems. Hydrogeol J 13:263–287

Güler C, Thyne GD, McCray JE, Turner AK (2002) Evaluation of graphical and multivariate statistical methods for classification of water chemistry data. Hydrogeol J 10:455–474

Han LF, Plummer LN, Aggarwal P (2014) The curved ^{14}C vs. $\delta^{13}C$ relationship in dissolved inorganic carbon: a useful tool for groundwater age and geochemical interpretations. Chem Geol 387:111–125

Hchaichi Z, Abid K, Zouari K (2014) Use of hydrochemistry and environmental isotopes for assessment of groundwater resources in the intermediate aquifer of the Sfax basin (southern Tunisia). Carbonates Evaporites 29:177–192

He JH, Ma JZ, Zhang P, Tian LM, Zhu GF, Edmunds WM, Zhang QH (2012) Groundwater recharge environments and hydrogeochemical evolution in the Jiuquan Basin, Northwest China. Appl Geochem 27:866–878

Herczeg AL, Edmunds WM (2000) Inorganic ions as tracers. Springer, New York

Huang P, Wang Z (2010) Impact of human activity on groundwater recharge in Shule River basin, Northwest China. AGU Fall Meet Abstr 1:1057

Huang TM, Pang ZH, Edmunds M (2013) Soil profile evolution following land-use change: implications for groundwater quantity and quality. Hydrol Process 27:1238–1252

Ingerson E, Pearson FJ (1964) Estimation of age and rate of motion of ground water by the ^{14}C method. In: Recent researches in the fields of hydrosphere. Atmos Nucl Chem 263–283

Keeling CD, Piper SC, Bacastow RB, Wahlen M, Whorf TP, Heimann M, Meijer HA (2005) Atmospheric CO_2 and $^{13}CO_2$ exchange with the terrestrial biosphere and oceans from 1978 to 2000: observations and carbon cycle implications. In: Ehleringer JR, Cerling TE,

Dearing MD (eds) A history of atmospheric CO_2 and its effects on plants, animals, and ecosystems. Springer, New York, pp 83–113

Landmeyer JE, Stone PA (1995) Radiocarbon and $\delta^{13}C$ values related to ground water recharge and mixing. Ground Water 33(2):227–234

Li JJ, Wen S, Zhang Q (1979) Study on the times, extent and form of Tibet plateau upheaving (in Chinese). Sci China 9:608–616

Li WZ, Yan P, Liu YG, Ding LG (2011) Phreatic water recharged source on the northeast of Kumtag Desert (in Chinese). J Desert Res 31(6):1617–1622

Lis GP, Wassenaar LI, Hendry MJ (2008) High precision laser spectroscopy D/H and measurements of microliter natural water samples. Anal Chem 80(1):287–293

Liu YP, Yamanaka T (2012) Tracing groundwater recharge sources in a mountain–plain transitional area using stable isotopes and hydrochemistry. J Hydrol 464:116–126

Liu JR, Song XF, Yuan GF, Sun XM, Liu X, Chen F, Wang ZM, Wang SQ (2008) Characteristics of $\delta^{18}O$ in precipitation over Northwest China and its water vapor sources. Acta Geograph Sin 63(1):12–22

Lloyd JW, Heathcote JA (1985) Natural inorganic hydrochemistry in relation to groundwater. Oxford University Press, New York

Luoma S, Okkonen J, Korkka-Niemi K, Hendriksson N, Backman B (2015) Confronting the vicinity of the surface water and sea shore in a shallow glaciogenic aquifer in southern Finland. Hydrol Earth Syst Sci 19(3):1353–1370

Ma JZ, Edmunds WM (2006) Groundwater and lake evolution in the Badain Jaran Desert ecosystem, Inner Mongolia. Hydrogeol J 14: 1231–1243

Ma JZ, Edmunds WM, He JH, Jia B (2009) A 2000 year geochemical record of palaeoclimate and hydrology derived from dune sand moisture. Paleogeogr Paleoclimatol Paleoecol 276:38–46

Ma JZ, Pan F, Chen LH, Edmunds WM, Ding ZY, He JH, Zhou KP, Huang TM (2010) Isotopic and geochemical evidence of recharge sources and water quality in the Quaternary aquifer beneath Jinchang City, NW China. Appl Geochem 25:996–1007

Ma JZ, He JH, Qi S, Zhu GF, Zhao W, Edmunds WM, Zhao YP (2013) Groundwater recharge and evolution in the Dunhuang Basin, Northwestern China. Appl Geochem 28:19–31

Mendizabal I, Stuyfzand PJ, Wiersma AP (2011) Hydrochemical system analysis of public supply well fields, to reveal water-quality patterns and define groundwater bodies: The Netherlands. Hydrogeol J 19(1):83–100

Meyer B, Tapponnier P, Metivier F, Bourjot L, Gaudemer Y, Peltzer G, Guo SM, Chen ZT (1998) Crustal thickening in Gansu-Qinghai, lithospheric mantle subduction, and oblique, strike-slip controlled growth of the Tibet plateau. Geophys J Int 135:1–47

Mook WG (1976) The dissolution-exchange model for dating groundwater with ^{14}C. In: Interpretation of environmental isotope and hydrochemical data in groundwater hydrology. IAEA, Vienna, pp 213–225

Münnich KO (1957) Messung des ^{14}C-Gehalts von hartem Grundwasser [Measurement of the ^{14}C content of hard groundwater]. Naturwissenschaften 44:32–39

Nimmo JR, Healy RW, Stonestrom DA (2005) Aquifer recharge. In: Anderson MG, Bear J (eds) Encyclopedia of hydrological science, vol 4. Wiley, Chichester, UK, pp 2229–2246

Okkonen J, Kløve B (2012) Assessment of temporal and spatial variation in chemical composition of groundwater in an unconfined esker aquifer in the cold temperate climate of northern Finland. Cold Reg Sci Technol 71:118–128

Parkhurst DL, Appelo CAJ (1999) User's guide to PHREEQC (Version 2): a computer program for speciation, batch-reaction, one-dimensional transport, and inverse geochemical calculations. US Geol Surv Water Resour Invest Rep 310:99–4259

Pophare AM, Lamsoge BR, Katpatal YB, Nawale VP (2014) Impact of over-exploitation on groundwater quality: a case study from WR-2 Watershed, India. J Earth Syst Sci 123(7):1541–1566

Qu JX, Yu SB (2007) The transformation relationship and chemical characteristics of the surface water and groundwater in the Shule River basin (in Chinese). Gansu Sci Technol 23(4):119–121

Ray RK, Mukherjee R (2008) Reproducing the piper trilinear diagram in rectangular coordinates. Groundwater 46(6):893–896

Sarah S, Ahmed S, Boisson A, Violette S, Marsily GD (2014) Projected groundwater balance as a state indicator for addressing sustainability and management challenges of over exploited crystalline aquifers. J Hydrol 519:1405–1419

Scanlon BR, Healy RW, Cook PG (2002) Choosing appropriate techniques for quantifying groundwater recharge. Hydrogeol J 10:18–39

Scherberg J, Baker T, Selker JS, Henry R (2014) Design of managed aquifer recharge for agricultural and ecological water supply assessed through numerical modeling. Water Resour Manag 28(14):4971–4984

Schoeller H (1965) Hydrodynamique dans le karst [Hydrodynamics of karst]. Actes du Colloques de Doubronik. IAHS/UNESCO, Wallingford, UK/Paris, pp 3–20

Schot PP, van der Wal J (1992) Human impact on regional groundwater composition through intervention in natural flow patterns and changes in land use. J Hydrol 134:297–313

Simmers I (1997) Recharge of phreatic aquifers in (semi)-arid areas. IAH International Contributions to Hydrogeology, 19A.A. Balkema, Rotterdam, pp 19–98

StatSoft (1995) STATISTICA for Windows, 1995, vol III: statistics II, 2nd edn. StatSoft, Tulsa, OK, pp 3197–3234

Tamers MA (1975) Validity of radiocarbon dates on groundwater. Geophys Surv 2:217–239

Tapponnier P, Meyer B, Avouac JP, Peltzer G, Gaudemer Y, Guo SM, Xiang HF, Yin KL, Chen ZT, Cai SH, Dai HG (1990) Active thrusting and folding in the Qilian Mountains, and decoupling between upper crust and mantle in northeastern Tibet. Earth Planet Sci Lett 97:382–403

Vogel JC (1967) Investigation of groundwater flow with radiocarbon. In: Isotopes in hydrology. IAEA, Vienna, pp 255–368

Vogel JS, Nelson DE, Southon JR (1987) C-14 background levels in an accelerator mass spectrometry system. Radiocarbon 29(3):323–333

Wada Y, van Beek LPH, van Kempen CM, Reckman JWTM, Vasak S, Bierkens MFP (2010) Global depletion of groundwater resources. Geophys Res Lett 37(20), L20402

Wang G, Han J, Zhou L, Xiong X, Wu Z (2005a) Carbon isotope ratios of plants and occurrence of C4 species under different soil moisture regimes in arid region of North West China. Physiol Plant 125:74–81

Wang JH, Liao KT, E YZ, Su ZZ, Zhai XW, Liu HJ, Tang JN, Ding F, Zhang JC, Zheng QZ (2005b) Preliminary results of the comprehensive scientific investigation in the Kumtag Desert (in Chinese). Gansu Sci Technol 21(10):6–8

Wang NL, Zhang SB, He JQ, Pu JC, Wu XB, Jiang X (2009) Tracing the major source area of the mountainous runoff generation of the Heihe River in Northwest China using stable isotope technique. Chin Sci Bull 54:2751–2757

Wang P, Yu JJ, Zhang YC, Liu CM (2013) Groundwater recharge and hydrogeochemical evolution in the Ejina Basin, Northwest China. J Hydrol 476:72–86

Ward JH (1963) Hierarchical grouping to optimize an objective function. J Am Stat Assoc 69:236–244

Xia J, Zhang L, Liu CM, Yu JJ (2007a) Towards better water security in North China. Water Resour Manag 21(1):233–247

Xia X, Wang F, Zhao Y (2007b) Lop Nur in China (in Chinese). Science Press, Beijing, pp 3–5

Zhao LJ, Lin L, Xiao HL, Cheng GD, Zhou MX, Yang YG, Li CZ, Zhou J (2011) Isotopic evidence for the moisture origin and composition of surface runoff in the headwaters of the Heihe River Basin. Chin Sci Bull 56:406–416

Zhu GF, Su YH, Feng Q (2008) The hydrochemical characteristics and evolution of groundwater and surface water in the Heihe River Basin, Northwest China. Hydrogeol J 16:167–182